Investigation physical properties of sprayed Cr doped ZnO thin films

A. M. Saleh[a,*], M. O. Dawood[b], S. S. Chiad[c], Z. S. A. Mosab[d], N. F. Habubi[e]
[a]*Department of Physics, College of Education, University of Garmian, Iraq*
[b]*Department of Physics, College of Science, Mustansiriyah University, Baghdad, Iraq*
[c]*Department of Physics, College of Education, Mustansiriyah University, Baghdad, Iraq*
[d]*Department of Pharmacy, Al-Manara College for Medical Science, Iraq*
[e]*Department of Radiation and Sonar Technologies, Alnukhba, University College, Baghdad, Iraq*

ZnO and ZnO:Cr films were grown by the chemical spray deposition (CSD). The effect of the Cr content on ZnO was studied. All ZnO films show polycrystalline, hexagonal wurtzite structure, with (002) dominant plane. AFM displayed that films have a compact surface, its root mean square roughness increased with Cr percentage. The average diameter was smaller than 64 nm. The optical bandgap was evaluated using Transmittance data. Their values were found to be decreases via increment in Cr doping.

(Received August 31, 2023; Accepted November 21, 2023)

Keywords: CSD, ZnO: Cr thin films, XRD, AFM and UV-Vis spectrophotometer

1. Introduction

ZnO possesses direct bandgap of 3.37eV and n-type conductivity [1-3]. (ZnO) is a transparent conducting oxide (TCO) material that has garnered significant attention due to its desirable properties. Thin films of ZnO are particularly attractive for various applications[4, 5]. One key advantage is their exceptional chemical and mechanical stability, especially in environments involving hydrogen plasma. This makes ZnO thin films suitable for use in harsh conditions where other materials may deteriorate [6-8]. It is employed in variety of applications, like UV light emitters [9], piezoelectric transducers [10] and gas sensors [11]. Cr doping can ameliorate the gas sensor properties of ZnO films [12]. The ionic radius of Cr^{+3} (0·63 Å) is nearer to Zn^{+2} (0·74 Å) [13]. Several deposition methods were used to grow ZnO films, including PLD [14], RF plasma [15], SPD [16], electrochemical [17], spin-coating [18], and dip coating [19-21]. Among these methods, spray pyrolysis stands out as a particularly attractive option due to several advantageous characteristics. First and foremost, spray pyrolysis is known for its cost-effectiveness, making it a financially viable choice for many applications. Additionally, this technique is relatively simple and straightforward to implement, requiring minimal complexity in equipment and setup [22, 23]. That dopants can act as a deviation in lattice parameter [24]. This work investigates the nanostructures of ZnO thin film synthesis by SPD at different Cr doping.

2. Experimental

Zinc oxide was obtained by melting (0.1M) of Zn $(CH_3COO)_2$. $2H_2O$ in redistilled water. Few drops of acetic acid were added to ban the formation of $Zn(OH)_2$. The mixed solution was whiskered at 50°C for 90 min to be fine and transparent. For Cr doping, 0.1 M of Chromium (II) chloride was dissolved in redistilled water to get 2% and 4% Cr doped ZnO. The substrates are glass slides cleaned with acetone via ultrasonic bath. The resultant solution was sprayed onto

* Corresponding author: adnan.mahmud@garmian.edu.krd
https://doi.org/10.15251/JOR.2023.196.663

preheated substrate retained at 400 oC. N^2 was employed as transporter gas, flow rate was 4 ml/min, distance between spout -base was 28 cm, spray time was 7 s followed by 1.5 wait to prevent substrate cooling. Film thickness was carried out by weighing method, 300 ± 30 nm. Transmittance spectra were recorded using double beam spectrophotometer. XRD and AFM were used to obtain a structural and topographical characterization.

3. Results and discussion

Figure 1 offers XRD styles of pure ZnO and (1, 3) % Cr doping in ZnO thin films deposited at 400ºC. All the samples were hexagonal polycrystalline, with a dominant peak along (002). The XRD patterns of these samples agrees with ICDD (No. 36-1451) data [25]. The high intensity of the (002) peak in all the spectra indicated good quality of films [26]. The three distinguished peaks are displayed in the Figure 1, conformable to ZnO (002), (100) and (101) reflections.

The average crystalline size (D) of grown films was evaluated by Scherrer's equation 1 [27-29]:

$$D = \frac{0.94\lambda}{\beta cos\theta} \tag{1}$$

where λ is the wavelength of X-ray, β is FWHM. D of the grown films is about (16.84-27.37) nm [30]. As we can notice from Table 1 that, Cr content improves crystalline quality.

The dislocation density (δ) is predestined by utilizing D by the relations [31-33]:

$$\delta = \frac{1}{D^2}\left(\frac{lines}{m^2}\right) \tag{2}$$

The microstrain (ε) is also predestined by utilizing D by the 3 relations [34-36]:

$$\varepsilon = \frac{\beta cos\theta}{4}(lines^{-2}.m^{-1}) \tag{3}$$

The estimated values are displayed in Table 1. The peaks intensity of doped films is increased compared to ZnO, showing a tiny variation in lattice parameters via Cr content [37].

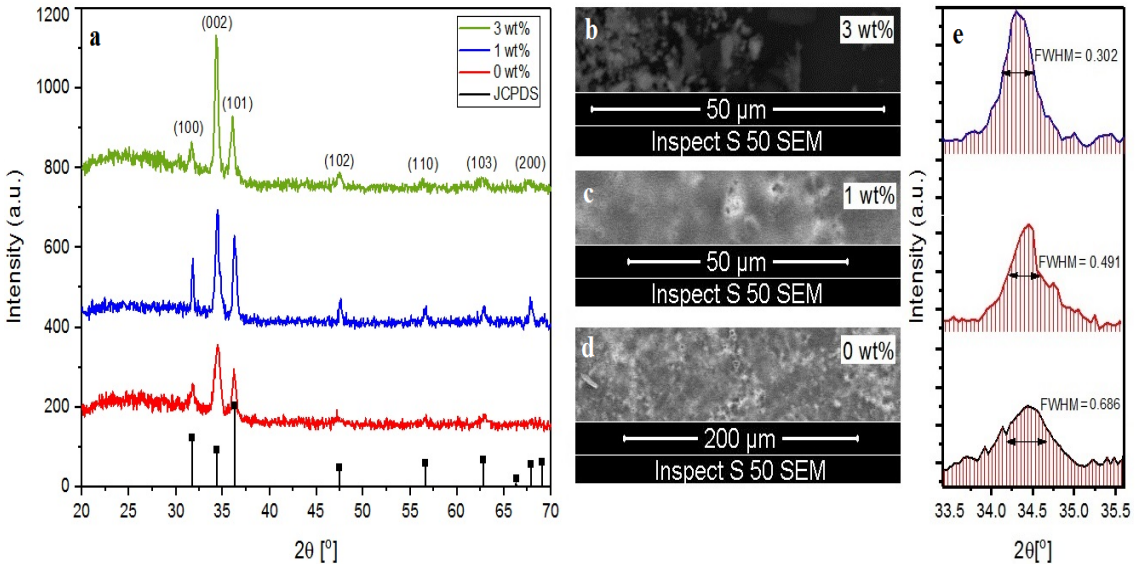

Fig. 1. XRD patterns of the deposited films.

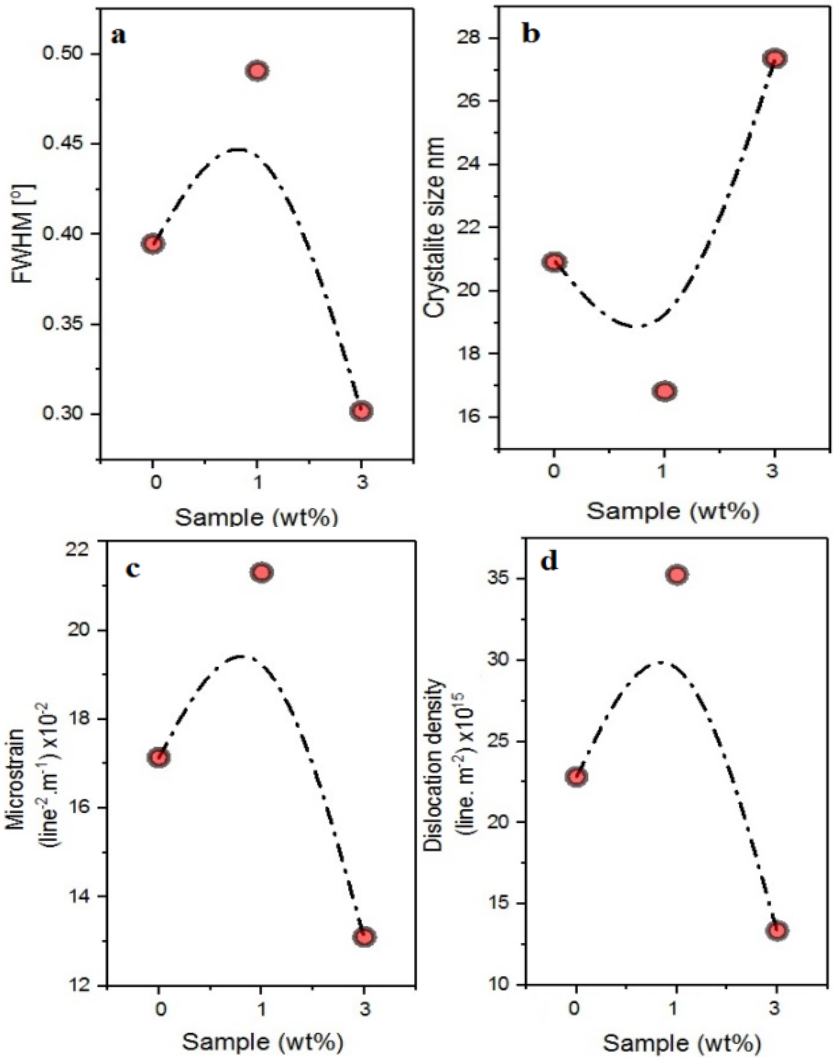

Fig. 2. Structural parameter of the deposited films.

Table 1. Structural data of intended films.

Sample (wt %)	(hkl) Plane	2theta (Deg.)	Lattice Constanta (Å)	FWHM (Rad)	Crystalite size D (nm)	Microstrain (line^{-2}.m^{-1})× 10^{-3}	Dislocation density(δ) (line.m^{-2})×10^{15}
0	(002)	34.44	3.249	0.395	20.93	1.71	2.28
1	(002)	34.44	3.249	0.491	16.84	2.13	3.53
3	(002)	34.44	3.249	0.302	27.37	1.31	1.33

Figure (3-5) represents a two-dimensional SEM image for undoped ZnO 1% Cr doped ZnO, 3% Cr doped ZnO respectively.

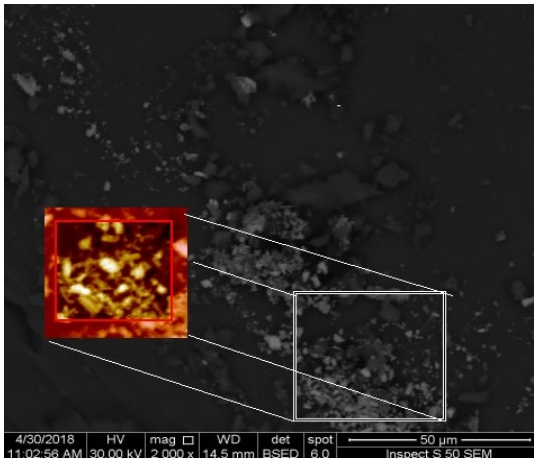

Fig .3. SEM image for undoped ZnO.

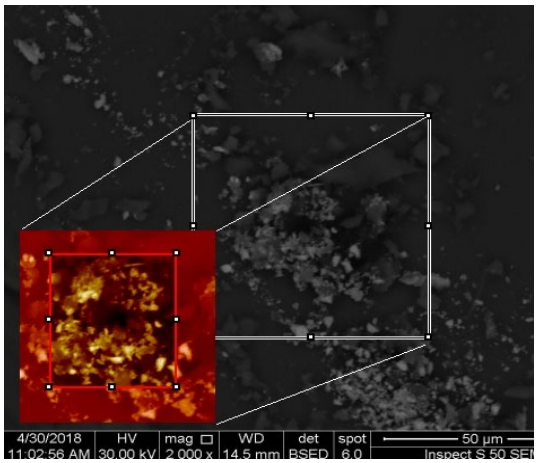

Fig. 4. SEM image for 1% Cr doped ZnO.

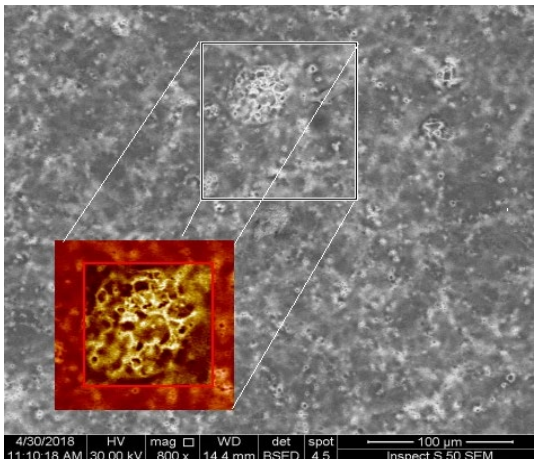

Fig. 5. SEM image for 3% Cr doped ZnO.

4. AFM analysis

Figure 6 presents AFM images of ZnO:Cr films, revealing a uniformly smooth surface for all samples. However, variations in surface morphology were observed, which can be attributed to different molar compositions of the dopant. As the Cr content increased, the crystal quality of the films decreased. The inclusion of transition metal ions in the ZnO lattice impeded nucleation and hindered the further growth of ZnO grains. The surface roughness values were found to increase with higher Cr concentration. This can be attributed to an increase in nucleation centers number, leading to an elevation in surface roughness.

Moreover, the introduction of Cr in ZnO films results in an increased presence of defects, further contributing to roughness and deterioration in surface distribution. Table 2 provides the values of RMS (root mean square) and average diameter, indicating a rough surface with an increase in diameter. Similar findings have been reported by Chang et al. [38, 39].

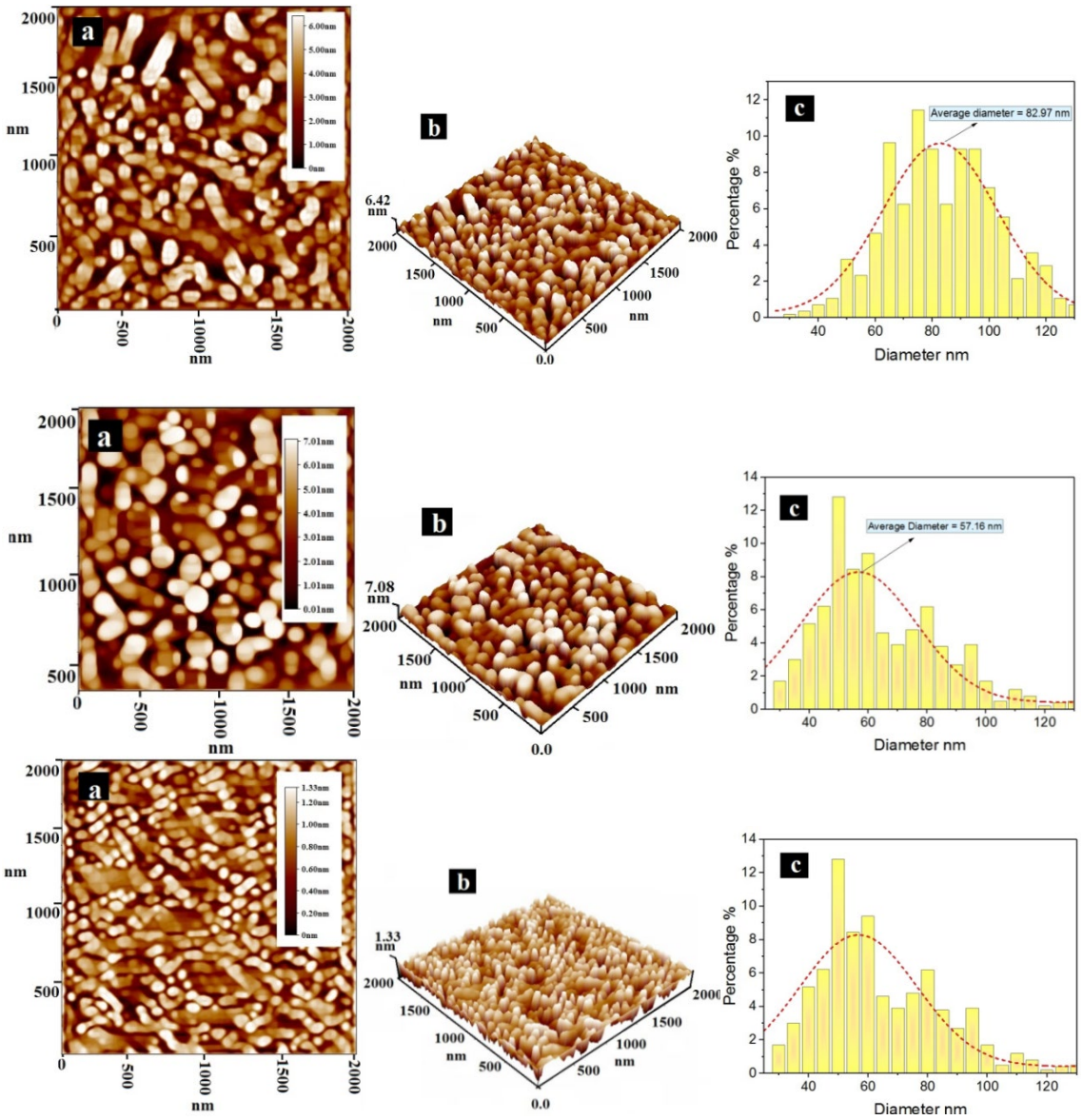

Fig. 6. AFM images (a, b , c) RMS, Roughness Average and Avg. Diameter, of the deposited films.

Table 3. Surface morphology of ZnO with different Cr doping by (SPD).

Samples (wt %)	Average particle size (nm)	Average roughness (nm)	RMS (nm)
0	57.16	0.25	0.303
1	53.12	1.68	1.96
3	82.97	1.4	1.66

5. Optical properties

Transmittance spectra of the deposited films grown at various doping concentrations are displayed in Fig. 7. The transmittance value was 50 - 80 % in the wavelength area 500-900 nm. Film transmittance was increased via doping, possibly due to improved film stoichiometry or by lowering defects [40, 41].

The absorption coefficient (α) can be determined using Equation (4) [42-44]

$$\alpha = 2.303(A/T) \tag{4}$$

Figure 7 illustrates the relationship between α and the photon energy. It can be observed that αgradually increases at longer wavelengths and then sharply rises near the absorption edge. This behavior indicates that the value of α is influenced by the doping of Chromium (Cr). Moreover, the absorption coefficient decreases as the Cr content increases [45, 46].

α with photon energy (hν) is utilized to evaluate energy bandgap E_g. The direct transition is expressed by Equation 1 [47-49]:

$$(\alpha h\nu) = B\left(h\nu - E_g\right)^n \tag{5}$$

where B is a constant.

A values are set to increase with the increase of doping from 1% to 3% as displayed in Fig. 8, this could be attributed to ZnO's white color does not absorb visible light. But with Cr^{+3} ions showing a replacement with Zn^{+2} ions , Zn ions absorb light in the visible region [50, 51].

The bandgap of ZnO was set to 3.25 eV. While the bandgap of the doped was 3.15 eV to 3.13 eV. These result were agreed with references [52, 53].

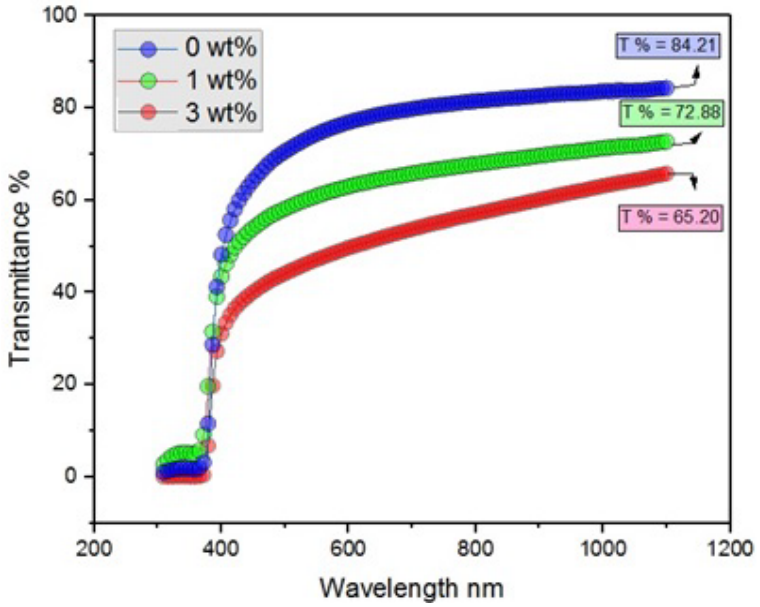

Fig. 7. Transmittance of the deposited films.

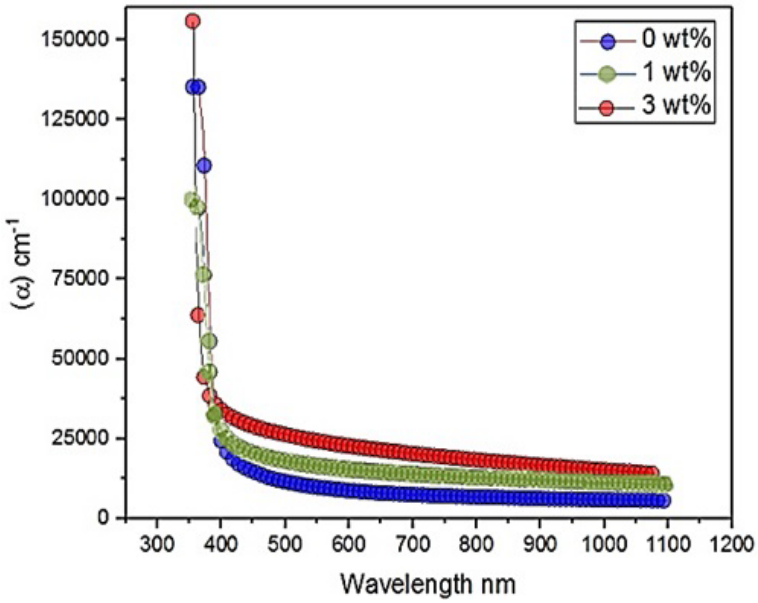

Fig. 8. α of the deposited films.

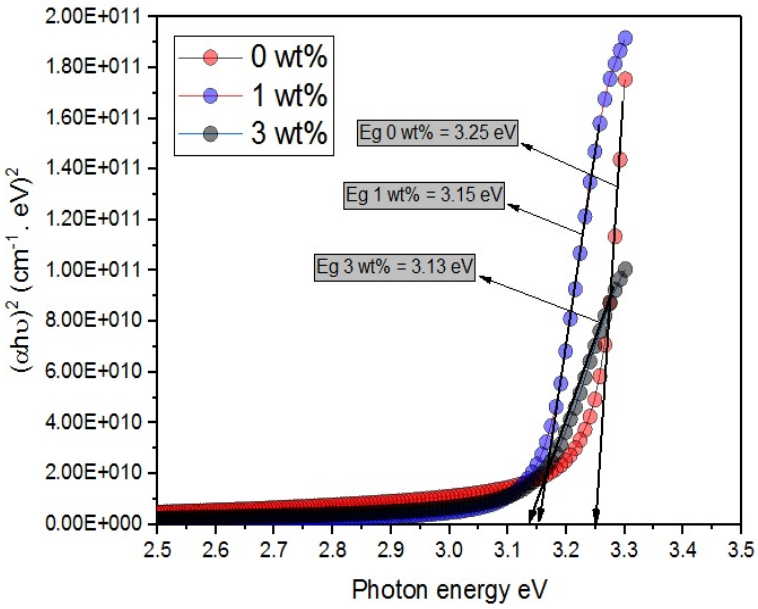

Fig. 9. Bandgap energy of the deposited films.

6. Conclusion

The ZnO and Cr/ZnO films with different doping was successfully prepared. crystallite sizes decreased slightly with increasing Cr dopant. The AFM results show that the surface roughness values increased with the increment in Cr, and the average diameter was smaller than 75 nm. Optical bandgap decreased with Cr doping, while absorption coefficient values increased.

Acknowledgements

This work was backed via Mustansiriyah University (www.uomustansiriyah.edu.iq) and Alnukhba University College. The author is grateful to the research lab at the College of Education, University of Garmian.

References

[1] Y. Yan, R. Lim, and J. M. White, Journal of Applied Physics, 106 (7), 074512 (2009); https://doi.org/10.1063/1.3236663
[2] H. K. Yadav, K. Sreenivas, V. Gupta, Journal of Applied Physics, 107(4), 044507 (2010); https://doi.org/10.1063/1.3291133
[3] C. Jin, A. Tiwari, R. J. Narayan, Journal of Applied Physics, 98(8), 083707 (2005); https://doi.org/10.1063/1.2108156
[4] C. Bundesmann, N. Ashkenov, M. Schubert, D. Spemann, T. Butz, E. M .Kaidashev, M. Lorenz, M. Grundmann, Applied Physics Letters, 83(10),1974–1976 (2003); https://doi.org/10.1063/1.1609251
[5] Y. S. Kim, W. P. Tai, S. J. Shu, Thin Solid Films, 491(1),153–160 (2005); https://doi.org/10.1016/j.tsf.2005.06.013.
[6] H. Liu, V Avrutin, N. Izyumskaya, U. Ozgur, H. Morkoc, Superlattices and Microstructures, 48(5):458–484, 2010. https://doi.org/10.1016/j.spmi.2010.08.011.
[7] J. Orozco-Messana, R. Daly, I. F. Zanchetta-Chittka, ceramics international, 46 (16), 24831-24837 (20200; https://doi.org/10.1016/j.ceramint.2020.06.229
[8] M. K. Singha, A. Patra, V. Rojwal, K. G. Deepa, and D. Kumar AIP Conference Proceedings, 2082(1), 030023 (2019); https://doi.org/10.1063/1.5093841.
[9] D. Ariosa, F. Elhordoy, E. A. Dalchiele, R. E. Marotti, C. Stari, Journal of Applied Physics, 110(12), 124901 (2011); https://doi.org/10.1063/1.3669026.
[10] X. Zhang, S. Ma, F. Li, F. Yang, J. Liu, Q. Zhao, Journal of Alloys and Compounds, 574, 149–154, (2013); https://doi.org/10.1016/j.jallcom.2013.04.055.
[11] A. Kolodziejczak-Radzimska, E. Markiewicz, T. Jesionowski. Journal of Nanomaterials, 2012, 2012. https://doi.org/10.1155/2012/656353.
[12] R. E. Marotti, D. N. Guerra, C. Bello, G. Machado, E. A. Dalchiele, Solar Energy Materials and Solar Cells, 82 (1–2), 85-1032004 (2004); https://doi.org/10.1016/j.solmat.2004.01.008
[13] Y. Lee, H. Kim, Y. Roh, Japanese Journal of Applied Physics, 40, 2423–2428 (2001); https://doi.org/10.1143/JJAP.40.2423.
[14] S. Singh, E. S. Kumar and M. S. R. Rao, Scripta Materialia, 58, 866–869 (2008); https://doi.org/10.1016/j.scriptamat.2008.01.008
[15] T. Sato, H. Suzuki, O. Kido, M. Kurumada, K. Kamitsuji, Y. Kimura, H. Kawasaki, S. Kaneko, Y. Saito and C. Kaito, J. Crystal Growth, 275, e983–e987 (2005); https://doi.org/10.1016/j.jcrysgro.2004.11.152
[16] Raid A.Ismail, Yassen Najim and Mohammad O. dawood, , e-J. Surf. Sci. Nanotech. Vol. 6 96-98 (2008); https://doi.org/10.1380/ejssnt.2008.96
[17] Jun Yang, Yongqian Wang, Junhan Kong, Hanxiang Jia, Zhengshu Wang, optical materials, 46, 179-185 (2015); https://doi.org/10.1016/j.optmat.2015.04.016
[18] V. Sharma, P. Kumar, J. Shrivastava, A. Solanki, V. R. Satsangi, S. Dass and R. Shrivastav, Int. J. Hydrogen Energy, 36, 4280–4290 (2011); https://doi.org/10.1016/j.ijhydene.2011.01.004
[19] A. E. Kandjani, M. F. Tabriz, O. M. Moradi, H. R. R. Mehr, S. A. Kandjani and M. R. Vaezi, J. Alloys Compounds, 509, 7854–7860 (2011); https://doi.org/10.1016/j.jallcom.2011.01.133
[20] F. D. Paraguay,W. L. Estrada, D. R. Acosta, E. Andrade, M. M.Yoshida, Thin Solid Films, 350 (1), 192–202 (1999); https://doi.org/10.1016/S0040-6090(99)00050-4.
[21] N. Kalyani, Y. C. Ching, and N. Azizi. Materials Research Innovations, 18(sup6):126–130, (2014); https://doi.org/10.1179/1432891714Z.0000000001013.
[22] P. Singh, A. Kumar, X. Deepak, and D. Kaur., Journal of Crystal Growth, 306 (2) 303–310 (2007); https://doi.org/10.1016/j.jcrysgro.2007.05.023.

[23] S. Edinger, J. Bekacz, M. Richter, R. Hamid, R. Wibowo, A. Peic, T. Dimopoulos, Thin Solid Films, 594:238–244, (2015); https://doi.org/10.1016/j.tsf.2015.04.027.
[24] R. Bhargava, P. K. Sharma, S. Kumar, A. C. Pandey and N. Kumarm, J. Solid State Chem.,183,1400–1408 (2010); https://doi.org/10.1016/j.jssc.2010.04.014
[25] Z. Sofiani, B. Derkowska, P. Dalasiński, M. Wojdyła, S. Dabos-Seignon, M. Alaoui Lamrani, L. Dghoughi, W. Bała, M. Addou, B. Sahraoui, optics communications, 267 (2), 433-439 (2006); https://doi.org/10.1016/j.optcom.2006.06.049
[26] F. D. Paraguay,W. L. Estrada, D. R. Acosta, E. Andrade, M. M.Yoshida, Thin Solid Films, 350 (1), 192–202 (1999); https://doi.org/10.1016/S0040-6090(99)00050-4.
[27] E. S. Hassan, A.K. Elttayef, S.. Mostafa, M. H. Salim, S.S. Chiad, Journal of Materials Science: Materials in Electronics, 30 (17), 15943-15951, (2019); https://doi.1007/s10854-019-01954-1
[28] E. H. Hadi, D. A. Sabur, S. S. Chiad, N. F. Habubi, K., Abass, Journal of Green Engineering, 10 (10), 8390-8400 (2020); https://doi.org/10.1063/5.0095169
[29] D. M. A. Latif, S. S. Chiad, M. S. Erhayief, K. H. Abass, N. F. Habubi, H. A. Hussin, Journal of Physics, Conference Series 1003(1) 012108 (2018); https://doi.org/10.1088/1742-6596/1003/1/012108
[30] S. Edinger, J. Bekacz, M. Richter, R. Hamid, R. Wibowo, A. Peic, T. Dimopoulos. Thin Solid Films, 594:238–244, (2015); https://doi.org/10.1016/j.tsf.2015.04.027.
[31] M. D. Sakhil, Z. M. Shaban, K. S. Sharba, N. F. Habub, K. H. Abass, S. S. Chiad, A. S. Alkelaby, NeuroQuantology, 18 (5), 56-61 (2020); https://doi.org/10.14704/nq.2020.18.5.NQ20168
[32] A. J. Ghazai, O. M. Abdulmunem, K. Y. Qader, S. S. Chiad, N. F. Habubi, AIP Conference Proceedings 2213 (1), 020101 (2020); https://doi.org/10.1063/5.0000158
[33] H. A. Hussin, R. S. Al-Hasnawy, R. I. Jasim, N. F. Habubi, S. S. Chiad, Journal of Green Engineering, 10(9)7018-7028 (2020); https://doi.org/10.1088/1742-6596/1999/1/012063
[34] E. S. Hassan, A. K. Elttayef, S. H. Mostafa, M. H. Salim and S. S. Chiad. Journal of aterials Science: Materials in Electronics, 30 (17),15943-15951 (2019); https://doi.org/10.1155/2014/684317
[35] R. S. Ali, H. S. Rasheed, N. F. Habubi, S.S. Chiad, Lettersthis link is disabled, 20(1), 63–72 (2023; https://doi.org/10.15251/CL.2023.201.6
[36] M. S. Othman, K. A. Mishjil, H. G. Rashid, S. S. Chiad, N. F. Habubi, I. A. Al-Baidhany, Journal of Materials Science: Materials in Electronics, 31(11), 9037-9043 (2020); https://doi.org/10.1007/s10854-020-03437-0
[37] Xu W Z, Ye Z Z, Zeng Y J, Zhu L P, Zhao B H, Jiang L, Lu J G, He H P and Zhang S B, Appl.Phys. Lett. 88 173506 (2006); https://doi.org/10.1063/1.2199588
[38] Olvera, M.d.l.L., et al., Journal of Materials Science: Materials in Electronics, 11(1): 1-5 (2000); https://doi.org/10.1023/A;100897380554
[39] R.-C. Chang, S.-Y. Chua, P.-W. Yeh, Sensors and Actuators, B132, 290–295 (2008); https://doi.org/10.1016/j.snb.2008.01.038
[40] N. Kalyani, Y C Ching, and N Azizi. Materials Research Innovations, 18(6):126–130, (2014); https://doi.org/10.1179/1432891714Z.0000000001013.
[41] P. Singh, A. Kumar, X. Deepak, and D. Kaur,Journal of Crystal Growth, 306 (2) 303–310 (2007); https://doi.org/10.1016/j.jcrysgro.2007.05.023.
[42] H. T. Salloom, E. H. Hadi, N. F. Habubi, S. S. Chiad, M. Jadan, J. S. Addasi, Digest Journal of Nanomaterials and Biostructures, 15 (4), 189-1195 (2020); https://doi.org/10.15251/DJNB.2020.154.1189
[43] R. S. Ali, M. K. Mohammed, A. A. Khadayeir, Z. M. Abood, N. F. Habubi and S. S. Chiad, Journal of Physics: Conference Series, 1664 (1), 012016 (2020); https://doi:10.1088/1742-6596/1664/1/012016
[44] S. S. Chiad, H. A. Noor, O. M. Abdulmunem, N. F. Habubi, M. Jadan, J. S. Addasi, Journal of Ovonic Research, 16 (1), 35-40 (2020).
[45] E. S. Hassan, T. H. Mubarak, K.H. Abass, S. S. Chiad, N. F. Habubi, M. H. Rahid, A. A. Khadayeir, M. O. Dawod, I. A. Al-Baidhany, Journal of Physics: Conference Series, 1234(1), 012013 (2019); https://doi.org/10.1088/1742-6596/1234/1/012013

[46] R. S. Ali, K. S. Sharba, A. M. Jabbar, S. S. Chiad, K. H. Abass, N. F. Habubi, NeuroQuantology 18 (1) 26-31 (2020); https://doi.org/10.14704/nq.2020.18.1.NQ20103
[47] N. N. Jandow, M. S. Othman, N. F.Habubi, S. S. Chiad, K. A. Mishjil, I. A. Al-Baidhany, Materials Research Express, 6 (11), (2020); https://doi.org/10.1088/2053-1591/ab4af8
[48] E. S. Hassan, K. Y. Qader, E. H. Hadi, S. S. Chiad, N. F. Habubi, K. H. Abass, Nano Biomedicine and Engineering, 12(3), pp. 205-213 (2020); https://doi.org/10.5101/nbe.v12i3.p205-213
[49] R. S Ali, N. A. H. Al Aaraji, E. H. Hadi, N. F. Habubi, S. S. Chiad, Journal of Nanostructuresthis link is disabled, 10(4), 810–816 (2020); https://doi: 10.22052/jns.2020.04.014
[50] N. Y. Ahmed, B. A. Bader, M. Y. Slewa, N. F. Habubi, S. S. Chiad, NeuroQuantology, 18(6), 55-60 (2020); https://doi.org/10.14704/nq.2020.18.6.NQ20183
[51] A. A. Khadayeir, R. I. Jasim, S. H. Jumaah, N. F, Habubi, S. S. Chiad, Journal of Physics: Conference Series,1664 (1) (2020); https://doi.org/10.1088/1742-6596/1664/1/012009
[52] A. Ghazai, K. Qader, N. F. Hbubi, S. S. Chiad, O. Abdulmunem, IOP Conference Series: Materials Science and Engineering, 870 (1), 012027 (2020); https://doi.org/ 10.1088/1757-899X/870/1/012027
[53] B. Ergin, E. Ketenci, F. Atay, Characterization of ZnO films obtained by ultrasonic spray pyrolysis technique. International Journal of Hydrogen Energy, 34, 5249–5254 (2009); https://doi.org/10.1016/j.ijhydene.2008.09.108.